Effect of Calcination on the Sintering of Gel-Derived, Zirconia-Toughened Alumina

Peter den Exter,[†] Louis Winnubst[*,‡] Theo H. P. Leuwerink,[†] and Anthonie J. Burggraaf

University of Twente, Faculty of Chemical Technology, Laboratory of Inorganic Chemistry,
Materials Science and Catalysis, 7500 AE Enschede, The Netherlands

The densification behavior of ZrO_2 (+3 mol% Y_2O_3)/85 wt% Al_2O_3 powder compacts, prepared by the hydrolysis of metal chlorides, can be characterized by a transition- and an α-alumina densification stage. The sintering behavior is strongly determined by the densification of the transition alumina aggregates. Intra-aggregate porosity, resulting from calcination at 800°C, partly persists during sintering and alumina phase transformation and negatively influences further macroscopic densification. Calcination at 1200°C, however, densifies the transition alumina aggregates prior to sintering and enables densification to almost full density (96%) within 2 h at 1450°C, thus obtaining a microstructure with an alumina and a zirconia grain size of 1 μm and 0.3–0.4 μm, respectively.

I. Introduction

THE mechanical properties of alumina ceramics can be improved by dispersing 15 wt% zirconia in the alumina matrix.[1] The toughening mechanisms associated with zirconia-toughened alumina (ZTA) are related to the phase transformation from metastable tetragonal zirconia to the monoclinic form during cooling after sintering (microcrack toughening) or during mechanical loading (transformation toughening).

High strength and toughness require an optimized transformation-toughening mechanism. This can be achieved by sintering to dense, fine-grained ceramics with zirconia grain sizes less than the critical grain size for spontaneous transformation $(0.7 \ \mu m)^2$ and by further applying postsintering heat treatments to obtain the proper fraction of transformable zirconia. An alumina grain $\leq 1 \ \mu m$ after sintering has the added advantage of making hot forging possible as a postsintering heat treatment.[3]

A range of wet-chemical techniques have been reported for the preparation of zirconia–alumina ceramic powders[4–10] which result in fine-grained transition alumina- (γ-, θ-Al_2O_3) containing powders with an intimate mixture of both zirconia and alumina. Transition aluminas are metastable and will transform to α-alumina during sintering. In all methods mentioned above, pressure-assisted sintering techniques were necessary to obtain dense materials.

The concept of simultaneous sintering and phase transformation was first reported by Badkar and Bailey[11] as an alternative processing route for the preparation of alumina ceramics. They observed a drastic decrease in densification rate upon the phase transformation to α-alumina, because the transformation to α-alumina is a nucleation and growth process. The densification behavior can be improved by a close control of the nucleation kinetics by seeding[12] or compaction.[13] The relation between nucleation kinetics and sintering behavior has now been well established.[14,15]

Literature strongly suggests that, apart from nucleation kinetics, a relation exists between the morphology of the transition alumina aggregates and the microstructural development during the phase transformation to α-alumina.[16] Although Dynys and Halloran[17] extensively studied the relation between the presence of α-alumina aggregates and the densification behavior, they did not take into consideration the morphology of the original transition alumina aggregates.

The aim of this paper is to investigate the influence of calcination temperature on the morphology of transition alumina aggregates and the sintering behavior of gel-derived ZTA compacts, and to establish the influence of zirconia on this part of the sintering process. In this way we expect to be able to obtain a microstructure after the alumina phase transformation, which provides a better opportunity for low-temperature sintering and optimum grain growth control than a more conventional approach on the basis of α-alumina.

II. Experimental Procedure

(1) Powder Preparation

ZrO_2 (+3 mol% Y_2O_3)/85 wt% Al_2O_3 powders were prepared by the hydrolysis of a dilute solution $(0.8M)$ of metal chlorides in HCl $(0.2M)$ by adding it slowly to a dispersion turbine reactor[18] with a large excess of NH_4OH (Merck, 25%). The hydrous gel was washed nine times in water/ammonia mixtures (pH ≥ 11) to remove all of the chloride. Between each washing step, the gel was allowed to settle, after which the clear supernatant liquid was removed. The gel was filtered and wet-milled with ethanol in polyethylene bottles using Teflon balls. Subsequently the gel was washed three times with ethanol to remove free water. The gel was dried in air at 120°C, dry-milled in a polyethylene bottle using Teflon balls, and calcined in air for 2 h at temperatures ranging from 550° to 1300°C (heating rate 2.5°C/min) to examine the influence of the calcination temperature on the morphology of the transition alumina aggregates.

(2) Characterization

The chemical composition of the calcined powders was determined by X-ray fluorescence spectrometry (PW 1410 spectrometer, Philips, Eindhoven, Netherlands). The silicon content was determined by the method described by Kruidhof.[19] Minor elements were determined by atomic absorption spectroscopy.

The phase composition of the powders was determined by X-ray diffraction (PW 1710 X-ray diffractometer, Philips) with Cu$K\alpha$ radiation. The temperature of the phase transformation to α-alumina was measured in N_2, at 2.5°C/min, by differential scanning calorimetry, (DSC 1500, Stanton Redcroft, London, U.K.) using α-alumina as a reference. Crystallite size was determined from X-ray line broadening. The peak profiles of the

(111)-reflection of both tetragonal zirconia (JCPDS—card 17-923) and θ-alumina (JCPDS—card 23-1009) and the (400)-reflection of γ-alumina (JCPDS—card 10-425) were scanned stepwise (step size/measuring time = 0.015°/10 s) while the sample was rotated about the normal axis. The crystallite size was calculated using the Scherrer equation:[20]

$$D = \frac{K\lambda}{\beta \cos(\theta)} \qquad (1)$$

where D is the crystallite diameter, λ is the wavelength of the radiation, θ is the diffraction angle, K is a constant, and β is the integral line width corrected for instrumental broadening and $K\alpha$ separation. The calculations were based on the width at half maximum instead of the integral line width. Therefore, K was 0.94. The crystallite size and shape were also determined by transmission electron microscopy (200 CT, JEOL, Tokyo, Japan).

The pore structures were derived from the shape of the nitrogen adsorption/desorption isotherms, measured at $-196°C$ after degassing at 300°C (ASAP 2400, Micromeritics, Norcross, GA). The specific surface area of the powders was determined by nitrogen adsorption, using the same equipment.

Powders were isostatically pressed (400 MPa) and pressureless sintered for 2 h at 1600°C. Nonisothermal sintering behavior was investigated in a dilatometer (402E dilatometer, Netzsch, Exton, PA) at 2.5°C/min. Bulk densities of the green and sintered compacts were determined in Hg by the Archimedes technique. The broadening of the X-ray reflections did not justify an accurate calculation of the lattice parameters. All densities are therefore based upon the theoretical density of α-alumina (3.965 g/cm^3) and yttria-stabilized tetragonal zirconia (6.04 g/cm^3). The theoretical densities of the composites were calculated using the equation

$$\rho_{th} = \frac{100}{\left(\dfrac{X}{3.965}\right) + \left(\dfrac{Y}{6.04}\right)} \qquad (2)$$

where X and Y are the amount of alumina and zirconia, respectively.

The ceramic microstructure of polished and thermally etched ceramics was examined by scanning electron microscopy (JSM-35CF scanning electron microscope, JEOL). Grain sizes were measured by the line intercept technique.[21]

III. Results and Discussion

(1) Powder Properties

The hydrolysis of metal chlorides and subsequent calcination yields a powder which meets the required bulk-chemical composition. After calcination, the ZTA powders contained ≈ 500 ppm silicon, and the K_2O, CaO, and MgO concentrations were less than 100 ppm. The Fe_2O_3 content was less than 300 ppm and the Na_2O content less than 200 ppm.

With increasing calcination temperature (Table I), the alumina crystallization sequence, starting from bayerite $(Al(OH)_3)$ is

Bayerite $\rightarrow \eta/\gamma$-$Al_2O_3 \rightarrow \theta$-$Al_2O_3 \rightarrow \alpha$-$Al_2O_3$
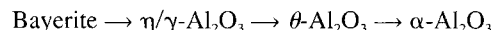
X-ray diffraction could not clearly distinguish between η- and γ-alumina, and thus they will be denoted as γ-alumina. In a pure alumina precursor, the transformation to α-alumina normally takes place at approximately 1150°C.[13] In gel-derived ZTA, the transformation to α-alumina is shifted toward a temperature above 1200°C. Likewise, tetragonal zirconia is not observed by X-ray diffraction until calcined at 800°C. In a pure yttria-doped zirconia precursor, tetragonal zirconia is observed when calcined at 550°C.[18] Apparently, zirconia and alumina strongly affect each other, indicating an intimate mixture of the phases.

The aggregate structure of the powder, as observed by transmission electron microscopy, reflects the morphology frequently observed for transition aluminas[16] and clearly consists of a stack of irregular alumina platelets with irregular slit-shaped pores separating the platelets. According to Wefers and Misra,[16] the actual structure of these pores is a combination of slit-shaped pores parallel to the (001) cleavage plane of the alumina and a network of irregularly shaped slits perpendicular to the (001) cleavage plane, thus giving rise to the irregularly shaped plate structure.

(2) Green Microstructure

A representative nitrogen adsorption–desorption isotherm on a ZTA compact, prepared from a powder calcined at 800°C, is given in Fig. 1. The hysteresis loop in the relative pressure range of 0.6 to 0.8, corresponding to a pore radius of 3 nm, typically results from wedge-shaped capillaries with a closed edge at the narrower side, perpendicular to open slit-shaped capillaries with parallel walls.[22] This type of hysteresis was also observed for the as-calcined powder and, thus, results from the intra-aggregate pore structure, as mentioned above.

The hysteresis loop, observed in the relative pressure range of 0.9 to 1.0, is of the A-type of De Boer's classification of isotherms[22] and corresponds to open capillaries with wide openings and narrow short necks and obviously results from interaggregate pores. Green compacts, prepared from powders calcined at a temperature >1000°C, have only A-type interaggregate pores, suggesting that the aggregates densified during calcination at a temperature somewhere between 1000° and 1100°C.

(3) Densification Behavior

Compacts prepared from powders calcined at temperatures ranging from 800° to 1200°C sinter to almost full density within 2 h at 1600°C (Table II). Two separate densification stages can

Table I. Characteristics of ZTA Powders after Calcination at Various Temperatures (T_{calc})

T_{calc} (°C)	Phase composition		$S_{B.E.T.}$ (m²/g)	Crystallite size (nm)	
	Al_2O_3	ZrO_2		ZrO_2	Al_2O_3
120	Bayerite	Amorph			
550	γ	Amorph	254		
800	γ	Tetr	126		6
900	θ	Tetr	83		6
1000	θ	Tetr/(monocl)	71		
1100	θ	Tetr	55	42–44*	33–35*
1200	θ	Tetr/(monocl)	32	33–48*	36–52*
1300	α	Tetr/(monocl)	6		

*Measured on several powder batches.
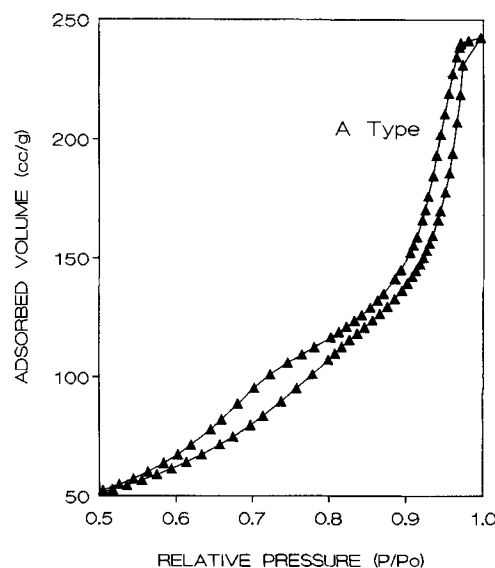

Fig. 1. Representative nitrogen adsorption–desorption isotherm on ZTA (T_{calc} = 800°C).

be distinguished (Fig. 2). The drastic decrease in densification rate at 1250°C is most likely caused by grain growth accompanying the alumina phase transformation at this temperature.[23] After the phase transformation, both compacts have a density of 51% of theoretical, as was calculated from the linear shrinkage.

The compact prepared from powder calcined at 1300°C contains α-alumina and cannot be sintered to a high density within 2 h at 1600°C (see Table II). The concept of simultaneous sintering and phase transformation thus provides a better opportunity for low-temperature sintering of ZTA-powder compacts than the more conventional approach on the basis of α-alumina.

After the alumina phase transformation, the compacts prepared from powders calcined at 800° and 1200°C show different densification behavior. The compact prepared from powder calcined at 1200°C densifies at a much lower temperature than the compact prepared from powder calcined at 800°C (Fig. 2). Compacts prepared from powder calcined at 550°C do not sinter to full density at all (Table II). Obviously, the final sintering temperature decreases with increasing calcination temperature.

It cannot be ruled out that calcination at a temperature as high as 1200°C for 2 h resulted in α-alumina nuclei, which because of their small amount could not be detected by X-ray diffraction. The formation of α-alumina nuclei during calcination may affect later transformation and densification behavior.[12–15] Although, on the basis of the difference in calcination temperature, different amounts of α-alumina nuclei should be expected, the densification behavior of compacts prepared from powders calcined at either 1100° or 1200°C did not show any difference. The influence of possible α-alumina nuclei can thus be left out. Any explanation for the observed difference in densification behavior of the compacts prepared from powders calcined at 800° and 1200°C should be found in a closer examination of the

microstructural development during densification and phase transformation.

Compacts prepared from powders calcined at 1200°C were also isothermally sintered at 1450°C. A density of more than 95% of theoretical is obtained within 2 h (Table II). Scanning electron microscopy demonstrated that after this heat treatment a homogeneous microstructure of equiaxed, 1.0-μm alumina grains was obtained. The zirconia is located on alumina grain boundaries and has a mean grain size of 0.3 to 0.4 μm.

To establish the influence of zirconia on the densification behavior, nonisothermal densification curves of both pure θ-alumina and ZTA compacts prepared from powders calcined at 900°C are given in Fig. 3. According to the densification curves, the alumina phase transformation in powder compacts is shifted from 1170° to 1240°C due to the presence of zirconia, which was confirmed by differential scanning calorimetry (DSC). The presence of zirconia, however, did not affect either the density directly after the transformation (51%) or the shape of the densification curve after the alumina phase transformation.

The observation that the phase transformation always takes place when the macroscopic density reached 51%, irrespective of calcination temperature or presence of zirconia, strongly suggests that a critical bulk density exists, above which the nucleation of α-alumina is not kinetically hindered and the alumina phase transformation takes place.

(4) Microstructural Development during Phase Transformation

The microstructural development during the θ- to α-alumina phase transformation obviously is the most important step during the densification of transition alumina-containing composites. The microstructural development during phase transformation was investigated by heating samples to a temperature just before or after the phase transformation and by subsequent cooling to room temperature. Just before the alumina phase transformation, the nitrogen adsorption/desorption isotherms of compacts prepared from powder calcined at 800°C still show a hysteresis loop in the relative pressure range below 0.9, representing intra-aggregate pores (Fig. 4). Apparently the aggregates did not sinter to full density during this stage of the sintering process.

After the phase transformation to α-alumina, the isotherm in the relative pressure range below 0.9 still shows some hysteresis (Fig. 4). This observation is in accordance with Wefers and Misra,[16] who state that the aggregate structure of irregularly shaped transition alumina platelets separated by irregularly shaped pores may persist during the phase transformation to α-alumina. The remaining hysteresis in the lower relative pressure range of the isotherm is ascribed to these pores.

Table II. Green Densities and Sintered Densities of Samples Prepared from ZTA Powders Calcined at Various Temperatures and Sintered at 1600°C for 2 h

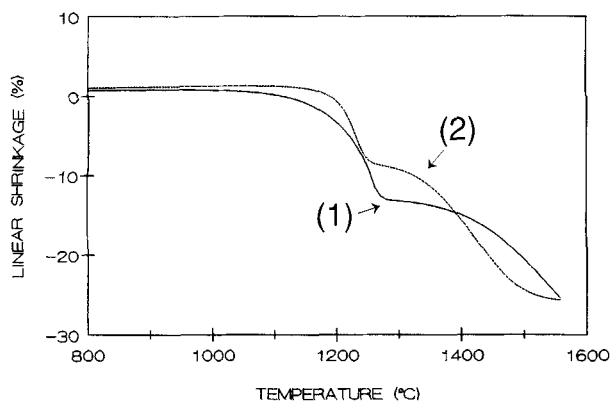| T_{cal} (°C)	ρ_{green} (%)	$\rho_{sintered}$ (%)
550	33	71
800	34	97
900	34	97
1000	36	98
1100	39	98
1200	40	98
1200	40	96*
1300	47	86

*Sintered for 2 h at 1450°C.

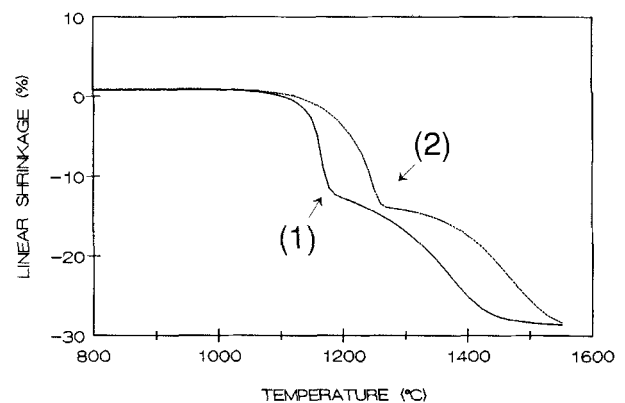Fig. 2. Dilatometer curve of ZTA calcined at 800°C (1) and 1200°C (2). Heating rate = 2.5°C/min.

Fig. 3. Dilatometer curve of pure θ-alumina (1) and ZTA (2). Calcination temperature = 900°C, heating rate = 2.5°C/min.
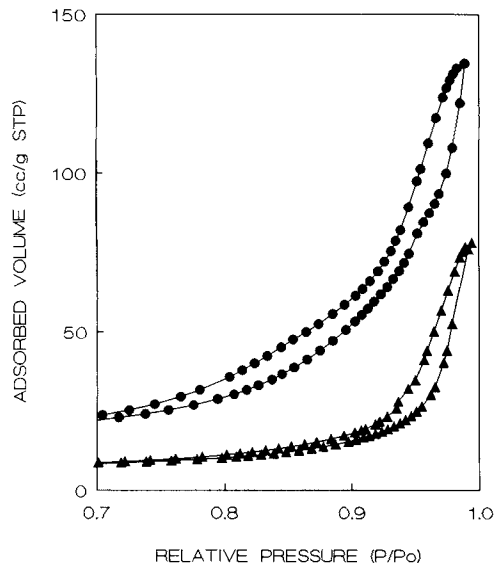
Fig. 4. Representative nitrogen adsorption–desorption isotherms on ZTA just before (●) and directly after (▲) the alumina phase transformation ($T_{calc} = 800°C$).

Just before the alumina transformation, the adsorption/desorption isotherm of the compact prepared from powder calcined at 1200°C showed no hysteresis which could be attributed to intra-aggregate pores, because the aggregates densified during calcination at 1200°C.

In contrast with the compact prepared from a powder calcined at 1200°C, considerable grain growth (from 6 to 34 nm) and a drastic decrease in specific surface area (from 118 to 40 m^2/g) are observed in the compact prepared from powder calcined at 800°C, during θ-alumina matrix sintering (Table III). Apparently both observations are related to the densification of the porous θ-alumina aggregates during sintering. Partial reduction of the specific surface area by pores' closing off and becoming undetectable by nitrogen adsorption, however, could not be completely ruled out. At the onset of alumina phase transformation ($T = 1220°C$), the compact prepared from powder calcined at 800°C still has a lower crystallite size and a higher specific surface area than the compact prepared from powder calcined at 1200°C, supporting the idea that the porous θ-alumina aggregates were still not completely densified at the onset of the phase transformation.

In the presence of zirconia, the alumina phase transformation takes place at a considerably higher temperature than in pure alumina (Fig. 3). The development of the pore size distribution of the pure alumina compact prepared from powder calcined at 900°C, during the alumina phase transformation, however, proved to be identical to that observed for ZTA compacts prepared from powder calcined at the same temperature. It looks as though zirconia decreases the densification rate of the transition

alumina aggregates; as a result, the assumed critical density at which the phase transformation takes place is reached at a later stage of the heating procedure.

The final sintering temperature of ZTA is related to the amount of densification of the transition alumina aggregates during calcination and sintering. Remaining porosity persists during the subsequent alumina phase transformation, thus giving rise to a microstructure which densifies only at a higher temperature. The higher sintering temperature is most likely to be caused by the presence of more irregularly shaped α-alumina particles. In this paper it is demonstrated that, by means of a proper selection of the calcination temperature of gel-derived ZTA powders, a dense microstructure after sintering can be obtained which meets the requirements mentioned in the introduction.

IV. Conclusions

ZrO_2 (+ 3 mol% Y_2O_3)/85 wt% Al_2O_3 powders were prepared by the hydrolysis of metal chlorides. The powders mainly contain porous transition alumina aggregates of which the porosity decreases with increasing calcination temperature.

The densification behavior of the powder compacts can be characterized by a transition- and an α-alumina densification stage, clearly separated by the alumina phase transformation.

The microstructural development during the transition alumina densification stage can be characterized by a further densification of the transition alumina aggregates.

When calcined at relatively low temperatures, the aggregates do not densify completely during the transition alumina densification stage. Remaining intra-aggregate porosity persists during the alumina phase transformation and negatively influences further densification.

Compacts prepared from powder calcined at 1200°C reach almost full density (96%) after sintering for 2 h at 1450°C, resulting in an alumina and a zirconia grain size of 1 μm and 0.3–0.4 μm, respectively.

References

[1]N. Claussen, "Fracture Toughness of Al_2O_3 with an Unstabilized ZrO_2 Dispersed Phase," *J. Am. Ceram. Soc.*, **59** [1–2] 49–51 (1976).

[2]E. Bischoff and M. Rühle, "Microcrack and Transformation Toughening of Zirconia-Containing Alumina"; pp. 635–43 in Advances in Ceramics, Vol. 24, *Science and Technology of Zirconia III*. Edited by S. Somiya, N. Yamamoto, and H. Yanagida. American Ceramic Society, Columbus, OH, 1988.

[3]Y. Maehara and T. G. Langdon, "Superplasticity in Ceramics," *J. Mater. Sci.*, **25**, 2275–86 (1990).

[4]J. C. Debsikdar, "Influence of Synthesis Chemistry on Alumina-Zirconia Powder Characteristics," *J. Mater. Sci.*, **22**, 2237–47 (1987).

[5]J. P. Bach and F. Thévenot, "Fabrication and Characterization of Zirconia-Toughened Alumina Obtained by Inorganic and Organic Precursors," *J. Mater. Sci.*, **24**, 2711–21 (1989).

[6]E. A. Pugar and P. E. D. Morgan, "Coupled Grain Growth Effects in Al_2O_3/10 vol% ZrO_2," *J. Am. Ceram. Soc.*, **69** [6] C-120–C-123 (1986).

[7]H. Yoshimatsu, H. Kawasaki, and A. Osaka, "Stability of Tetragonal ZrO_2 Phase in Al_2O_3 Prepared from Zr-Al Organometallic Compounds," *J. Mater. Sci.*, **23**, 332–36 (1988).

[8]J. McKittrick, G. Kalonji, and T. Ando, "Microstructural Control of Al_2O_3-ZrO_2 Ceramics through Rapid Solidification"; see Ref. 2, pp. 267–75.

[9]G. Kalonji, J. McKittrick, and L. W. Hobbs, "Applications of Rapid Solidification Theory and Practice to Al_2O_3-ZrO_2 Ceramics"; pp. 816–25 in Advances in Ceramics, Vol. 12, *Science and Technology of Zirconia II*. Edited by N. Claussen, M. Rühle, and A. Heuer. American Ceramic Society, Columbus, OH, 1984.

[10]S. Hori, M. Yoshimura, S. Sōmiya, and R. Takahashi, "Al_2O_3-ZrO_2 Ceramics Prepared from CVD Powders"; see Ref. 9, pp. 794–805.

[11]P. A. Badkar and J. E. Bailey, "The Mechanism of Simultaneous Sintering and Phase Transformation in Alumina," *J. Mater. Sci.*, **11**, 1794–806 (1976).

[12]M. Kumagai and G. L. Messing, "Enhanced Densification of Boehmite Sol–Gels by α-Alumina Seeding," *J. Am. Ceram. Soc.*, **67** [11] C-230–C-231 (1984).

[13]F. W. Dynys and J. W. Halloran, "Alpha Alumina Formation in Alum-Derived Gamma Alumina," *J. Am. Ceram. Soc.*, **65** [9] 442–448 (1982).

Table III. Crystallite Sizes and Specific Surface Areas of Zirconia-Toughened Alumina after Isostatic Compaction, Prior to (1220°C) and directly after the Phase Transformation to α-alumina during Nonisothermal Sintering (2.5°C/min)

	T_{calc} (°C)	Green compact	Prior to $\theta \rightarrow \alpha$	After $\theta \rightarrow \alpha$
ZrO_2 crystallite	800		43	50
size (nm)	1200	44	57	57
Al_2O_3 crystallite	800	6	34	>100
size (nm)	1200	37	47	>100
Specific surface	800	118	40	16
area (m^2/g)	1200	35	22	8

[14]M. Kumagai and G. L. Messing, "Controlled Transformation and Sintering of a Boehmite Sol–Gel by α-Alumina Seeding," *J. Am. Ceram. Soc.*, **68** [9] 500–505 (1985).

[15]G. L. Messing and M. Kumagai, "Low-Temperature Sintering of Seeded Sol–Gel-Derived, ZrO_2-Toughened Al_2O_3 Composites," *J. Am. Ceram. Soc.*, **72** [1] 40–44 (1989).

[16]K. Wefers and C. Misra, "Oxides and Hydroxides of Aluminum"; Alcoa Technical Paper No. 19, Revised. Alcoa Laboratories, 1987.

[17]F. W. Dynys and J. W. Halloran, "Influence of Aggregates on Sintering," *J. Am. Ceram. Soc.*, **67** [9] 596–601 (1984).

[18]M. A. C. G. Van de Graaf, J. H. H. Ter Maat, and A. J. Burggraaf, "Microstructure and Sintering Kinetics of Highly Reactive ZrO_2-Y_2O_3 Ceramics," *J. Mater. Sci.*, **20**, 1407–18 (1985).

[19]H. Kruidhof, "The Determination of Small Amounts of Aluminum and Silicon in Stabilized Zirconia Ceramics," *Anal. Chim. Acta*, **99**, 193–195 (1978).

[20]K. P. Klug and L. E. Alexander, *X-ray Diffraction Procedure for Polycrystalline and Amorphous Materials*; ch. 9, pp. 618–708. Wiley, New York, 1974.

[21]J. C. Wurst and J. A. Nelson, "Lineal Intercept Technique for Measuring Grain Size in Two-Phase Polycrystalline Ceramics," *J. Am. Ceram. Soc.*, **55** [2] 109 (1972).

[22]J. H. De Boer, "The Shapes of Capillaries"; pp. 68–94 in *The Structure and Properties of Porous Materials*, Proceedings of the Tenth Symposium of the Colston Research Society (Bristol, U.K., 1958). Edited by D. H. Everett and F. S. Stone. Butterworths Scientific Publications, London, U.K., 1958.

[23]P. den Exter, A. J. A. Winnubst and A. J. Burggraaf, "Sintering of ZTA at Low Temperatures through Transition Alumina Densification"; pp. 1377–81 in *Euro-Ceramics II*, Vol. 2, Proceedings of the Second European Ceramic Society Conference (Augsburg, Germany). Edited by G. Ziegler and H. Hausner. Deutsche Keramische Gesellshaft, Köln, Germany, 1991.   □